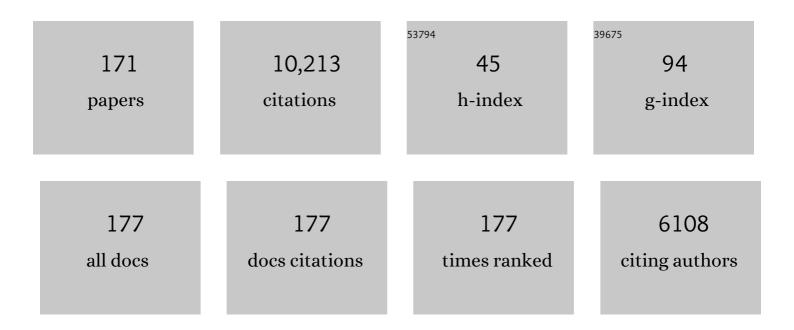
David Diner

List of Publications by Year in descending order

Source: https://exaly.com/author-pdf/1486562/publications.pdf Version: 2024-02-01



#	Article	IF	CITATIONS
1	Multi-angle Imaging SpectroRadiometer (MISR) instrument description and experiment overview. IEEE Transactions on Geoscience and Remote Sensing, 1998, 36, 1072-1087.	6.3	855
2	Synergistic algorithm for estimating vegetation canopy leaf area index and fraction of absorbed photosynthetically active radiation from MODIS and MISR data. Journal of Geophysical Research, 1998, 103, 32257-32275.	3.3	708
3	Multiangle Imaging Spectroradiometer (MISR) global aerosol optical depth validation based on 2 years of coincident Aerosol Robotic Network (AERONET) observations. Journal of Geophysical Research, 2005, 110, .	3.3	482
4	Multiangle Imaging SpectroRadiometer global aerosol product assessment by comparison with the Aerosol Robotic Network. Journal of Geophysical Research, 2010, 115, .	3.3	459
5	Techniques for the retrieval of aerosol properties over land and ocean using multiangle imaging. IEEE Transactions on Geoscience and Remote Sensing, 1998, 36, 1212-1227.	6.3	358
6	Smoke injection heights from fires in North America: analysis of 5 years of satellite observations. Atmospheric Chemistry and Physics, 2010, 10, 1491-1510.	4.9	280
7	MISR Aerosol Product Attributes and Statistical Comparisons With MODIS. IEEE Transactions on Geoscience and Remote Sensing, 2009, 47, 4095-4114.	6.3	256
8	Estimation of vegetation canopy leaf area index and fraction of absorbed photosynthetically active radiation from atmosphere-corrected MISR data. Journal of Geophysical Research, 1998, 103, 32239-32256.	3.3	251
9	Polarimetric remote sensing of atmospheric aerosols: Instruments, methodologies, results, and perspectives. Journal of Quantitative Spectroscopy and Radiative Transfer, 2019, 224, 474-511.	2.3	224
10	Wildfire smoke injection heights: Two perspectives from space. Geophysical Research Letters, 2008, 35, .	4.0	219
11	Structure and meteorology of the middle atmosphere of Venus: Infrared remote sensing from the Pioneer Orbiter. Journal of Geophysical Research, 1980, 85, 7963-8006.	3.3	214
12	New Directions in Earth Observing: Scientific Applications ofMultiangle Remote Sensing. Bulletin of the American Meteorological Society, 1999, 80, 2209-2228.	3.3	204
13	Analysis of Multi-angle Imaging SpectroRadiometer (MISR) aerosol optical depths over greater India during winter 2001-2004. Geophysical Research Letters, 2004, 31, .	4.0	199
14	Using angular and spectral shape similarity constraints to improve MISR aerosol and surface retrievals over land. Remote Sensing of Environment, 2005, 94, 155-171.	11.0	195
15	Comparison of MISR and AERONET aerosol optical depths over desert sites. Geophysical Research Letters, 2004, 31, .	4.0	193
16	Aerosol source plume physical characteristics from space-based multiangle imaging. Journal of Geophysical Research, 2007, 112, .	3.3	193
17	The value of multiangle measurements for retrieving structurally and radiatively consistent properties of clouds, aerosols, and surfaces. Remote Sensing of Environment, 2005, 97, 495-518.	11.0	159
18	Comparison of coincident Multiangle Imaging Spectroradiometer and Moderate Resolution Imaging Spectroradiometer aerosol optical depths over land and ocean scenes containing Aerosol Robotic Network sites. Journal of Geophysical Research, 2005, 110, .	3.3	146

#	Article	IF	CITATIONS
19	MISR aerosol optical depth retrievals over southern Africa during the SAFARI-2000 Dry Season Campaign. Geophysical Research Letters, 2001, 28, 3127-3130.	4.0	139
20	Sensitivity of multiangle imaging to aerosol optical depth and to pure-particle size distribution and composition over ocean. Journal of Geophysical Research, 1998, 103, 32195-32213.	3.3	137
21	The inter-comparison of major satellite aerosol retrieval algorithms using simulated intensity and polarization characteristics of reflected light. Atmospheric Measurement Techniques, 2010, 3, 909-932.	3.1	136
22	Surface albedo retrieval from Meteosat: 1. Theory. Journal of Geophysical Research, 2000, 105, 18099-18112.	3.3	128
23	The Airborne Multiangle SpectroPolarimetric Imager (AirMSPI): a new tool for aerosol and cloud remote sensing. Atmospheric Measurement Techniques, 2013, 6, 2007-2025.	3.1	128
24	Extraction of spectral hemispherical reflectance (albedo) of surfaces from nadir and directional reflectance data. International Journal of Remote Sensing, 1987, 8, 1727-1746.	2.9	116
25	Dual-photoelastic-modulator-based polarimetric imaging concept for aerosol remote sensing. Applied Optics, 2007, 46, 8428.	2.1	109
26	Decadal-scale trends in regional aerosol particle properties and their linkage to emission changes. Environmental Research Letters, 2017, 12, 054021.	5.2	109
27	Canopy Structure Parameters Derived from Multi-Angular Remote Sensing Data for Terrestrial Carbon Studies. Climatic Change, 2004, 67, 403-415.	3.6	107
28	Retrieval of aerosol properties over land using MISR observations. , 2009, , 267-293.		104
29	Dynamics of fire plumes and smoke clouds associated with peat and deforestation fires in Indonesia. Journal of Geophysical Research, 2011, 116, .	3.3	100
30	Simultaneous retrieval of aerosol and surface properties from a combination of AERONET and satellite data. Remote Sensing of Environment, 2007, 107, 90-108.	11.0	97
31	An overview of the ORACLES (ObseRvations of Aerosols above CLouds and their intEractionS) project: aerosol–cloud–radiation interactions in the southeast Atlantic basin. Atmospheric Chemistry and Physics, 2021, 21, 1507-1563.	4.9	97
32	Coordinated airborne, spaceborne, and ground-based measurements of massive thick aerosol layers during the dry season in southern Africa. Journal of Geophysical Research, 2003, 108, n/a-n/a.	3.3	96
33	Introducing the 4.4 km spatial resolution Multi-Angle Imaging SpectroRadiometer (MISR) aerosol product. Atmospheric Measurement Techniques, 2020, 13, 593-628.	3.1	84
34	Intercomparison of satellite retrieved aerosol optical depth over ocean during the period September 1997 to December 2000. Atmospheric Chemistry and Physics, 2005, 5, 1697-1719.	4.9	82
35	Advances in multiangle satellite remote sensing of speciated airborne particulate matter and association with adverse health effects: from MISR to MAIA. Journal of Applied Remote Sensing, 2018, 12, 1.	1.3	79
36	A data-mining approach to associating MISR smoke plume heights with MODIS fire measurements. Remote Sensing of Environment, 2007, 107, 138-148.	11.0	75

#	Article	IF	CITATIONS
37	Surface albedo retrieval from Meteosat: 2. Applications. Journal of Geophysical Research, 2000, 105, 18113-18134.	3.3	73
38	First results from a dual photoelastic-modulator-based polarimetric camera. Applied Optics, 2010, 49, 2929.	2.1	69
39	Joint retrieval of aerosol and water-leaving radiance from multispectral, multiangular and polarimetric measurements over ocean. Atmospheric Measurement Techniques, 2016, 9, 2877-2907.	3.1	69
40	MISR Calibration and Implications for Low-Light-Level Aerosol Retrieval over Dark Water. Journals of the Atmospheric Sciences, 2005, 62, 1032-1052.	1.7	65
41	The sensitivity of CO and aerosol transport to the temporal and vertical distribution of North American boreal fire emissions. Atmospheric Chemistry and Physics, 2009, 9, 6559-6580.	4.9	63
42	Exploration of a Polarized Surface Bidirectional Reflectance Model Using the Ground-Based Multiangle SpectroPolarimetric Imager. Atmosphere, 2012, 3, 591-619.	2.3	63
43	Coupled retrieval of aerosol properties and land surface reflection using the Airborne Multiangle SpectroPolarimetric Imager. Journal of Geophysical Research D: Atmospheres, 2017, 122, 7004-7026.	3.3	63
44	Atmospheric transfer of radiation above an inhomogeneous non-Lambertian reflective ground—I. Theory. Journal of Quantitative Spectroscopy and Radiative Transfer, 1984, 31, 97-125.	2.3	61
45	PARAGON: An Integrated Approach for Characterizing Aerosol Climate Impacts and Environmental Interactions. Bulletin of the American Meteorological Society, 2004, 85, 1491-1502.	3.3	59
46	A multiangle imaging spectroradiometer for terrestrial remote sensing from the earth observing system. International Journal of Imaging Systems and Technology, 1991, 3, 92-107.	4.1	54
47	Temperature, Cloud Structure, and Dynamics of Venus Middle Atmosphere by Infrared Remote Sensing from Pioneer Orbiter. Science, 1979, 205, 65-67.	12.6	52
48	Vertical distributions and relationships of cloud occurrence frequency as observed by MISR, AIRS, MODIS, OMI, CALIPSO, and CloudSat. Geophysical Research Letters, 2009, 36, .	4.0	50
49	The MISR radiometric calibration process. Remote Sensing of Environment, 2007, 107, 2-11.	11.0	49
50	Intra-annual variations of regional aerosol optical depth, vertical distribution, and particle types from multiple satellite and ground-based observational datasets. Atmospheric Chemistry and Physics, 2018, 18, 11247-11260.	4.9	49
51	Performance of the MISR LAI and FPAR algorithm: a case study in Africa. Remote Sensing of Environment, 2003, 88, 324-340.	11.0	46
52	Example applications of the MISR INteractive eXplorer (MINX) software tool to wildfire smoke plume analyses. Proceedings of SPIE, 2008, , .	0.8	46
53	Pioneer 11 Infrared Radiometer Experiment: The Global Heat Balance of Jupiter. Science, 1975, 188, 472-473.	12.6	45
54	Response to "Toward unified satellite climatology of aerosol properties. 3. MODIS versus MISR versus AERONET― Journal of Quantitative Spectroscopy and Radiative Transfer, 2011, 112, 901-909.	2.3	45

#	Article	IF	CITATIONS
55	MISR observations of Etna volcanic plumes. Journal of Geophysical Research, 2012, 117, .	3.3	45
56	MISR Dark Water aerosol retrievals: operational algorithm sensitivity to particle non-sphericity. Atmospheric Measurement Techniques, 2013, 6, 2131-2154.	3.1	45
57	Atmospheric transfer of radiation above an inhomogeneous non-Lambertian reflective ground—II. Computational considerations and results. Journal of Quantitative Spectroscopy and Radiative Transfer, 1984, 32, 279-304.	2.3	44
58	Analysis of the MISR LAI/FPAR product for spatial and temporal coverage, accuracy and consistency. Remote Sensing of Environment, 2007, 107, 334-347.	11.0	41
59	Infrared Remote Sounding of the Middle Atmosphere of Venus from the Pioneer Orbiter. Science, 1979, 203, 779-781.	12.6	40
60	Multiangle remote sensing: Past, present and future. International Journal of Remote Sensing, 2000, 18, 83-102.	1.0	40
61	Multi-Angle Imager for Aerosols. Public Health Reports, 2017, 132, 14-17.	2.5	38
62	Estimating PM2.5 speciation concentrations using prototype 4.4â€km-resolution MISR aerosol properties over Southern California. Atmospheric Environment, 2018, 181, 70-81.	4.1	38
63	Intercomparison of desert dust optical depth from satellite measurements. Atmospheric Measurement Techniques, 2012, 5, 1973-2002.	3.1	37
64	Retrieving Aerosol Characteristics From the PACE Mission, Part 2: Multi-Angle and Polarimetry. Frontiers in Environmental Science, 2019, 7, .	3.3	37
65	New approach to the retrieval of AOD and its uncertainty from MISR observations over dark water. Atmospheric Measurement Techniques, 2018, 11, 429-439.	3.1	36
66	Potential of multiangular spectral measurements to characterize land surfaces: Conceptual approach and exploratory application. Journal of Geophysical Research, 2000, 105, 17539-17549.	3.3	35
67	Aerosol Data Sources and Their Roles within PARAGON. Bulletin of the American Meteorological Society, 2004, 85, 1511-1522.	3.3	33
68	A modified linear-mixing method for calculating atmospheric path radiances of aerosol mixtures. Journal of Geophysical Research, 1997, 102, 16883-16888.	3.3	31
69	Retrieving Aerosol Characteristics From the PACE Mission, Part 1: Ocean Color Instrument. Frontiers in Earth Science, 2019, 7, .	1.8	31
70	SPEX airborne spectropolarimeter calibration and performance. Applied Optics, 2019, 58, 5695.	1.8	31
71	An integrated multiangle, multispectral, and polarimetric imaging concept for aerosol remote sensing from space. , 2005, , .		30
72	Humanâ€caused fires limit convection in tropical Africa: First temporal observations and attribution. Geophysical Research Letters, 2015, 42, 6492-6501.	4.0	30

#	Article	IF	CITATIONS
73	Calibration and validation of Airborne Multiangle SpectroPolarimetric Imager (AirMSPI) polarization measurements. Applied Optics, 2018, 57, 4499.	1.8	30
74	Atmospheric transmittance from spacecraft using multiple view angle imagery. Applied Optics, 1985, 24, 3503.	2.1	29
75	Coupled Retrieval of Liquid Water Cloud and Aboveâ€Cloud Aerosol Properties Using the Airborne Multiangle SpectroPolarimetric Imager (AirMSPI). Journal of Geophysical Research D: Atmospheres, 2018, 123, 3175-3204.	3.3	28
76	Aerosol retrievals from different polarimeters during the ACEPOL campaign using a common retrieval algorithm. Atmospheric Measurement Techniques, 2020, 13, 553-573.	3.1	28
77	Intercomparison of airborne multi-angle polarimeter observations from the Polarimeter Definition Experiment. Applied Optics, 2019, 58, 650.	1.8	28
78	Aerosol optical depths over oceans: A view from MISR retrievals and collocated MAN and AERONET in situ observations. Journal of Geophysical Research D: Atmospheres, 2013, 118, 12,620.	3.3	27
79	Polar clearing in the Venus clouds observed from the Pioneer Orbiter. Nature, 1979, 279, 613-614.	27.8	26
80	Rotation of Venus's polar dipole. Nature, 1983, 305, 116-119.	27.8	26
81	A Correlated Multi-Pixel Inversion Approach for Aerosol Remote Sensing. Remote Sensing, 2019, 11, 746.	4.0	26
82	Aerosolâ€cloud interactions in ship tracks using Terra MODIS/MISR. Journal of Geophysical Research D: Atmospheres, 2015, 120, 2819-2833.	3.3	25
83	Influence of Aerosol Scattering on Atmospheric Blurring of Surface Features. IEEE Transactions on Geoscience and Remote Sensing, 1985, GE-23, 618-624.	6.3	24
84	An optimization approach for aerosol retrievals using simulated MISR radiances. Atmospheric Research, 2012, 116, 1-14.	4.1	23
85	Markov chain formalism for vector radiative transfer in a plane-parallel atmosphere overlying a polarizing surface. Optics Letters, 2011, 36, 2083.	3.3	22
86	Sensitivity of multi-angle photo-polarimetry to vertical layering and mixing of absorbing aerosols: Quantifying measurement uncertainties. Journal of Quantitative Spectroscopy and Radiative Transfer, 2011, 112, 2149-2163.	2.3	22
87	Remote sensing of the atmosphere of Mars using infrared pressure modulation and filter radiometry. Applied Optics, 1986, 25, 4232.	2.1	21
88	Direct imaging of nonsolar planets with infrared telescopes using apodized coronagraphs. Applied Optics, 1991, 30, 3253.	2.1	21
89	Angle of linear polarization images of outdoor scenes. Optical Engineering, 2019, 58, 1.	1.0	21
90	Satellite assessment of sea spray aerosol productivity: Southern Ocean case study. Journal of Geophysical Research D: Atmospheres, 2016, 121, 872-894.	3.3	20

#	Article	IF	CITATIONS
91	Integrating and Interpreting Aerosol Observations and Models within the PARAGON Framework. Bulletin of the American Meteorological Society, 2004, 85, 1523-1534.	3.3	19
92	Infrared imaging of Venus: 8–14 micrometers. Icarus, 1976, 27, 191-195.	2.5	18
93	Prospecting for planets in circumstellar dust: sifting the evidence from β Pictoris. Nature, 1986, 322, 436-438.	27.8	18
94	MISR radiometric uncertainty analyses and their utilization within geophysical retrievals. Metrologia, 1998, 35, 571-579.	1.2	18
95	Linearization of Markov chain formalism for vector radiative transfer in a plane-parallel atmosphere/surface system. Applied Optics, 2012, 51, 3491.	1.8	18
96	Assessment of MISR Cloud Motion Vectors (CMVs) Relative to GOES and MODIS Atmospheric Motion Vectors (AMVs). Journal of Applied Meteorology and Climatology, 2017, 56, 555-572.	1.5	18
97	Scientific Objectives, Measurement Needs, and Challenges Motivating the PARAGON Aerosol Initiative. Bulletin of the American Meteorological Society, 2004, 85, 1503-1510.	3.3	17
98	Observing earthquake-related dewatering using MISR/Terra satellite data. Eos, 2003, 84, 37-43.	0.1	16
99	Multiscale Plume Transport from the Collapse of the World Trade Center on September 11, 2001. Environmental Fluid Mechanics, 2006, 6, 425-450.	1.6	16
100	Quantifying aerosol direct radiative effect with Multiangle Imaging Spectroradiometer observations: Topâ€ofâ€atmosphere albedo change by aerosols based on land surface types. Journal of Geophysical Research, 2009, 114, .	3.3	16
101	Markov chain formalism for generalized radiative transfer in a plane-parallel medium, accounting for polarization. Journal of Quantitative Spectroscopy and Radiative Transfer, 2016, 184, 14-26.	2.3	16
102	Toward Cloud Tomography from Space Using MISR and MODIS: Locating the "Veiled Core―in Opaque Convective Clouds. Journals of the Atmospheric Sciences, 2021, 78, 155-166.	1.7	16
103	Multi-angle Imaging SpectroRadiometer (MISR) time-lapse imagery of tsunami waves from the 26 December 2004 Sumatra–Andaman earthquake. Remote Sensing of Environment, 2007, 107, 256-263.	11.0	15
104	Analysis of static and time-varying polarization errors in the multiangle spectropolarimetric imager. Applied Optics, 2011, 50, 2080.	2.1	15
105	Photopolarimetric Sensitivity to Black Carbon Content of Wildfire Smoke: Results From the 2016 ImPACTâ€PM Field Campaign. Journal of Geophysical Research D: Atmospheres, 2018, 123, 5376-5396.	3.3	15
106	Calibration Plans for the Multi-angle Imaging SpectroRadiometer (MISR). Metrologia, 1993, 30, 213-221.	1.2	14
107	Three-dimensional radiative transfer using a fourier-transform matrix-operator method. Journal of Quantitative Spectroscopy and Radiative Transfer, 1985, 34, 133-148.	2.3	12
108	Planning for a spaceborne Earth Observation mission: From user expectations to measurement requirements. Environmental Science and Policy, 2015, 54, 419-427.	4.9	12

#	Article	IF	CITATIONS
109	Spectral Invariance Hypothesis Study of Polarized Reflectance With the Ground-Based Multiangle SpectroPolarimetric Imager. IEEE Transactions on Geoscience and Remote Sensing, 2019, 57, 8191-8207.	6.3	12
110	Using the PARAGON Framework to Establish an Accurate, Consistent, and Cohesive Long-Term Aerosol Record. Bulletin of the American Meteorological Society, 2004, 85, 1535-1548.	3.3	11
111	Radiometric stability of the Multi-angle Imaging SpectroRadiometer (MISR) following 15 years on-orbit. , 2014, , .		11
112	The MISR Calibration Program. Journal of Atmospheric and Oceanic Technology, 1996, 13, 286-299.	1.3	10
113	Refinements to MISR's radiometric calibration and implications for establishing a climate-quality aerosol observing system. , 2004, 5652, 57.		10
114	Linearization of a scalar matrix operator method radiative transfer model with respect to aerosol and surface properties. Journal of Quantitative Spectroscopy and Radiative Transfer, 2013, 116, 1-16.	2.3	10
115	Regional Changes in Earth's Color and Texture as Observed From Space Over a 15-Year Period. IEEE Transactions on Geoscience and Remote Sensing, 2016, 54, 4240-4249.	6.3	10
116	The Aerosol Characterization from Polarimeter and Lidar (ACEPOL) airborne field campaign. Earth System Science Data, 2020, 12, 2183-2208.	9.9	10
117	Phase coverage of Venus during the 1975 apparition. Icarus, 1978, 36, 119-126.	2.5	9
118	Comparison of ground-based and spacecraft observations of the infrared emission from Venus: The nature of thermal contrasts. Icarus, 1982, 52, 301-319.	2.5	9
119	Spectral invariance hypothesis study of polarized reflectance with Ground-based Multiangle SpectroPolarimetric Imager (GroundMSPI). , 2015, , .		9
120	Preface to the MISR Special Issue. Remote Sensing of Environment, 2007, 107, 1.	11.0	8
121	Quantitative studies of wildfire smoke injection heights with the Terra Multi-angle Imaging SpectroRadiometer. , 2008, , .		8
122	Generalized radiative transfer theory for scattering by particles in an absorbing gas: Addressing both spatial and spectral integration in multi-angle remote sensing of optically thin aerosol layers. Journal of Quantitative Spectroscopy and Radiative Transfer, 2018, 205, 148-162.	2.3	8
123	Correlation of simultaneous ultraviolet (0.36 μm) and infrared (8 to 14 μm) images of Venus. Icarus, 1979, 38, 81-89.	2.5	7
124	Barotropic Instability with Divergence: Theory and Applications to Venus. Journals of the Atmospheric Sciences, 1990, 47, 1578-1588.	1.7	7
125	Airborne multiangle spectropolarimetric imager (AirMSPI) observations over California during NASA's polarimeter definition experiment (PODEX). Proceedings of SPIE, 2013, , .	0.8	7
126	Improving MISR AOD Retrievals With Low-Light-Level Corrections for Veiling Light. IEEE Transactions on Geoscience and Remote Sensing, 2018, 56, 1251-1268.	6.3	7

#	Article	IF	CITATIONS
127	Evaluation of sea salt aerosols in climate systems: global climate modeling and observation-based analyses*. Environmental Research Letters, 2020, 15, 034047.	5.2	7
128	Can multi-angular polarimetric measurements in the oxygen-A and B bands improve the retrieval of aerosol vertical distribution?. Journal of Quantitative Spectroscopy and Radiative Transfer, 2021, 270, 107679.	2.3	7
129	Silicon vidicon imaging of jupiter. Icarus, 1977, 32, 299-313.	2.5	6
130	<title>Reflectance stability analysis of Spectralon diffuse calibration panels</title> . , 1991, , .		6
131	WindCam and MSPI: two cloud and aerosol instrument concepts derived from Terra/MISR heritage. Proceedings of SPIE, 2008, , .	0.8	6
132	Oceanic Aerosol Loading Derived From MISR's 4.4 km (V23) Aerosol Product. Journal of Geophysical Research D: Atmospheres, 2019, 124, 10154-10174.	3.3	6
133	Tomographic reconstruction of an aerosol plume using passive multiangle observations from the MISR satellite instrument. Geophysical Research Letters, 2016, 43, 12,590.	4.0	5
134	Aerosol profiling using radiometric and polarimetric spectral measurements in the O2 near infrared bands: Estimation of information content and measurement uncertainties. Remote Sensing of Environment, 2021, 253, 112179.	11.0	5
135	Estimating surface orientation from microfacet Mueller matrix bidirectional reflectance distribution function models in outdoor passive imaging polarimetry. Optical Engineering, 2019, 58, 1.	1.0	5
136	<title>Development status of the EOS Multiangle Imaging SpectroRadiometer (MISR)</title> . , 1993, 1939, 94.		4
137	<title>Spectroradiometer focal-plane design considerations: lessons learned from MISR camera testing</title> . , 1995, 2583, 104.		4
138	Applying a microfacet model to polarized light scattering measurements of the Earth's surface. , 2015, ,		4
139	Ten years of MISR observations from Terra: Looking back, ahead, and in between. , 2010, , .		3
140	Capabilities and limitations of MISR aerosol products in dust-laden regions. Proceedings of SPIE, 2011, ,	0.8	3
141	Addendum to "Generalized radiative transfer theory for scattering by particles in an absorbing gas: Addressing both spatial and spectral integration in multi-angle remote sensing of optically thin aerosol layers―[J. Quant. Spectrosc. Radiat. Transfer 205 (2018) 148–162]. Journal of Quantitative Spectroscopy and Radiative Transfer. 2018. 206. 251-253.	2.3	3
142	Novel airborne imaging polarimeter undergoes flight testing. SPIE Newsroom, 0, , .	0.1	3
143	COMPARATIVE ASPECTS OF VENUS AND TERRESTRIAL METEOROLOGY. Weather, 1981, 36, 34-41.	0.7	2
144	A sub-millimetre aperture synthesis array for nonsolar planet detection. Nature, 1989, 337, 51-53.	27.8	2

#	Article	IF	CITATIONS
145	Extrasolar planet detection. Astrophysics and Space Science, 1994, 212, 369-383.	1.4	2
146	<title>Instrument verification tests on the Multiangle Imaging Spectro-Radiometer (MISR)</title> . , 1997, , .		2
147	Current and future advances in optical multiangle remote sensing of aerosols and clouds based on Terra/MISR experience. , 2006, , .		2
148	Introducing the MISR level 2 near real-time aerosol product. Atmospheric Measurement Techniques, 2021, 14, 5577-5591.	3.1	2
149	AUTOMATED DATA PRODUCTION FOR A NOVEL AIRBORNE MULTIANGLE SPECTROPOLARIMETRIC IMAGER (AIRMSPI). International Archives of the Photogrammetry, Remote Sensing and Spatial Information Sciences - ISPRS Archives, 0, XXXIX-B1, 33-38.	0.2	2
150	EOS Multiangle Imaging Spectroradiometer. , 1990, , .		1
151	Multiangle Imaging of the Earth: Present and Future. , 2003, , .		1
152	Dust aerosol retrieval results from MISR. , 2004, , .		1
153	An Overview of Terra Mission Results Related to the Carbon Cycle. Geography Compass, 2009, 3, 536-559.	2.7	1
154	Looking back, looking forward: Scientific and technological advances in multiangle imaging of aerosols and clouds. AIP Conference Proceedings, 2017, , .	0.4	1
155	Polarimetric calibration of the multi-angle imager for aerosols (MAIA). , 2021, , .		1
156	Imaging Spectrometry In The Post-Eos Era. , 1989, , .		0
157	Exploitation of Surface Albedo Derived From the Meteosat Data to Characterize Land Surface Changes. Advances in Global Change Research, 2001, , 51-67.	1.6	Ο
158	Comments on: Retrieval of aerosol properties over the ocean using multispectral and multiangle photopolarimetric measurements from the research scanning polarimeter. Geophysical Research Letters, 2001, 28, 3275-3276.	4.0	0
159	Thermal Design and On-Orbit Performance of the Multi-Angle Imaging SpectroRadiometer. , 0, , .		Ο
160	PARAGON: A Systematic, Integrated Approach to Aerosol Observation and Modeling. , 2004, , .		0
161	Future Mission Concept for 3-D Remote Sensing of Aerosols from Low Earth Orbit. , 2007, , .		0
162	Future Mission Concept for Operational Retrieval of Cloud-Top Heights and Cloud Motion Wind		0

² Vectors., 2007, , .

#	Article	IF	CITATIONS
163	De-hazing of multi-spectral images with evolutionary computing. , 2010, , .		0
164	Challenges, solutions, and applications of accurate multiangle image registration: Lessons learned from MISR. , 0, , 355-382.		0
165	Mapping Speciated Ambient Particulate Matter Concentrations with the Multi-Angle Imager for Aerosols (MAIA). , 2018, , .		0
166	Water vapor retrieval using the Airborne Multiangle SpectroPolarimetric Imager. Journal of Quantitative Spectroscopy and Radiative Transfer, 2021, 267, 107610.	2.3	0
167	Reflected Solar Radiation Sensors, Polarimetric. Encyclopedia of Earth Sciences Series, 2014, , 663-668.	0.1	0
168	Reflected Solar Radiation Sensors, Multiangle Imaging. Encyclopedia of Earth Sciences Series, 2014, , 658-663.	0.1	0
169	Extrasolar Planet Detection. , 1994, , 369-383.		0
170	Polarization considerations in the multi-angle imager for aerosols (MAIA). , 2018, , .		0
171	Specifying polarimetric tolerances of a high-resolution imaging multiple-species atmospheric profiler (HiMAP). , 2019, , .		0